Associations of right ventricular myocardial function with skin and pulmonary involvement in asymptomatic patients with systemic sclerosis

Antonello D'Andrea, Salvatore Bellissimo*, Fortunato Scotto di Uccio, Francesco Vigorito, Francesco Moscato, Nicola Tozzi, Maria Di Donato, Rodolfo Citro**, Stefano Stisi*, Marino Scherillo

*Department of Interventional Cardiology and Coronary Care Unit, G. Rummo Hospital, *Department of Rheumatology, G. Rummo Hospital, Benevento, **Department of Cardiology, San Luca Hospital, Vallo della Lucania (SA), Italy*

Key words:
Diastole; Doppler myocardial imaging; Pulmonary hypertension; Right ventricle; Systemic sclerosis.

Background. **Systemic sclerosis (SSc) is a multisystem disorder characterized by widespread vascular lesions and fibrosis of the skin and specific internal organs. Cardiac involvement is a common finding in SSc, but often clinically occult. The aim of the present study was to analyze both left and right ventricular (RV) myocardial function in patients with SSc, and their relation to other instrumental features of the disease.**

Methods. **Twenty-five healthy subjects and 23 age- and sex-comparable asymptomatic patients classified as having either diffuse (11 patients) or limited cutaneous (12 patients) SSc underwent clinical examination, serological analysis, high-resolution chest computed tomography, standard Doppler echocardiography and pulsed Doppler myocardial imaging (DMI) of both the mitral and tricuspid annuli. SSc was classified using the modified Rodnan skin score (mRSS) into high mRSS (score ≥ 10) and low mRSS (score < 10).**

Results. **Serological antibody analysis revealed the presence of antinuclear antibody in all patients, an anticentromere pattern in 8 patients, and anti-Scl-70 antibodies in 15 patients. Eleven patients were diagnosed with interstitial pulmonary fibrosis at chest computed tomography. Standard Doppler echocardiography revealed that the left ventricular mass index and ejection fraction were comparable between the two groups, while the RV end-diastolic diameter was increased in SSc ($p < 0.01$). The tricuspid inflow peak E and E/A ratio were slightly decreased in SSc ($p < 0.01$), while the systolic pulmonary pressure was increased ($p < 0.0001$). DMI analysis revealed, in SSc, an impaired RV myocardial early-diastolic (E_m) peak velocity ($p < 0.001$) as well as a prolonged myocardial relaxation time (RT_m) ($p < 0.001$) only at the tricuspid annulus level, even after correction for age, sex, heart rate and left ventricular mass index. Independent inverse associations of the RV E_m peak velocity with both the Rodnan skin score (β coefficient = -0.62, $p < 0.0005$) and the pulmonary systolic pressure (β coefficient = 0.71, $p < 0.0001$), as well as the independent inverse correlation of the same RV E_m peak velocity with interstitial pulmonary fibrosis (odds ratio 0.68, 95% confidence interval 0.45-0.83, $p < 0.0005$) in SSc patients were assessed at multivariate analysis. In addition, the RV E_m velocity was an independent predictor of the anti-Scl-70 antibody pattern (odds ratio 0.68, 95% confidence interval 0.45-0.83, $p < 0.01$). Of note, a RV E_m peak velocity < 0.11 m/s well selected SSc patients with pulmonary artery pressure > 35 mmHg, pulmonary fibrosis, a high mRSS, and an anti-Scl-70 antibody pattern.**

Conclusions. **The relationships of RV myocardial diastolic dysfunction with both skin and pulmonary involvement as well as with the serological antibody pattern emphasizes the ability of DMI to identify patients with a more diffuse and severe form of SSc. This issue may be critical for the early identification of those SSc patients who are at higher risk of cardiac impairment, ideally when they are still asymptomatic before developing severe vasculopathy.**

(Ital Heart J 2004; 5 (11): 831-839)

Received May 26, 2004; revision received September 9, 2004; accepted September 14, 2004.

Address:
Dr. Antonello D'Andrea
Via G. Martucci, 35
80121 Napoli
E-mail:
adandrea@napoli.com

Systemic sclerosis (SSc), or scleroderma, is a systemic autoimmune disease characterized by vascular damage and fibrosis within the skin and visceral organs. Even though SSc is a heterogeneous disorder in terms of symptoms and clinical course, organ involvement is common, frequently affecting the kidneys, the gastrointestinal tract, the lungs and the heart[1-6].

The cardiac involvement in SSc is historically classified into primary and secondary. Primary heart disease depends on the involvement of the myocardium and microvasculature by the disease itself, with impairment of the global diastolic function and reduction of the coronary flow reserve, even in the absence of abnormalities of the epicardial coronary arteries[2,7,8]. Secondary

form of cardiac disease develops in SSc patients with vascular and/or interstitial lung disease, in which the fibrotic process leads to a marked reduction in the cross-sectional area of the pulmonary vascular bed due to obliteration of the alveolar capillaries and/or narrowing of many small arteries[5,6]. In both cases, the pathological hallmark of the cardiac impairment in SSc is myocardial fibrosis, which is mainly located in deposits within the interstitium[9-15].

The right ventricular (RV) chamber is often involved in systemic pathologies as a consequence of a direct injury extension, afterload changes or ventricular inter-dependence which is mainly due to the close anatomic association between the two ventricles[16,17]. However, this issue has not often been explored by means of non-invasive techniques because of the complexity of the RV geometry which precludes an accurate assessment of the dimensions of the RV chamber and their changes during the cardiac cycle[18-21]. Using standard Doppler echocardiography, other authors have pointed out an impaired RV filling in a significant percentage of SSc patients in whom no other cause of altered diastolic function had been detected[9,10,12]. To the best of our knowledge, no report describing both the left ventricular (LV) and RV regional myocardial involvement in such a systemic disease has been published to date.

The aim of the present study was therefore to analyze the systolic and diastolic myocardial function in patients with SSc, and their relation to other instrumental features of the disease, by means of Doppler myocardial imaging (DMI). This technique provides accurate information about the segmental myocardial motion during the cardiac cycle and offers the advantage, with respect to conventional Doppler echocardiography, of assessing the systolic and diastolic function of both ventricles at a regional level[22-26].

Methods

Study population. From an initial cohort of 56 patients with SSc, 23 asymptomatic patients classified as having either the diffuse (11 patients) or limited form (12 patients) of SSc, and 25 age- and sex-comparable healthy subjects were enrolled into the study after their informed consent and approval of the Ethics Committee of the G. Rummo Hospital were obtained. The exclusion criteria were: arterial hypertension, coronary artery disease (angina and/or ECG signs of myocardial ischemia), severe valvular heart disease, more than second degree mitral regurgitation, NYHA functional classes II, III and IV, atrial fibrillation, lung disease, and inadequate echocardiograms.

All patients underwent clinical examination, serological tests, high-resolution chest computed tomography (CT), standard Doppler echocardiography, and pulsed DMI of both the mitral and tricuspid annuli.

Procedures. Standard Doppler echocardiography and DMI were performed with the subjects in partial left decubitus, using the Acuson Sequoia ultrasound system (Mountain View, CA, USA) equipped with DMI capabilities. A variable frequency phased-array transducer (2.5-3.5-4.0 MHz) was used for two-dimensional, M-mode and Doppler imaging. Doppler echocardiographic and DMI tracings were recorded on a magneto-optical disk. All the measurements were analyzed by two experienced readers, who averaged the data of ≥ 3 cardiac cycles.

M- and B-mode. Two-dimensional measurements of the septal and posterior wall thickness were obtained at end-diastole, in the parasternal short-axis view and integrated with those obtained in the parasternal long-axis and apical views. Endocardial fractional shortening was calculated as: LVEDD - LVESD/LVEDD $\times$ 100 where LVEDD = LV end-diastolic diameter and LVESD = LV end-systolic diameter. LV mass was calculated in accordance with the Penn convention[27] using the following formula:

$$\text{LV mass (g)} = 1.04\,[(\text{LVEDD}+\text{IVST}+\text{PWT})^3 - (\text{LVEDD})^3] - 13.6$$

where IVST = interventricular septal thickness, PWT = posterior wall thickness. LV mass was indexed for height$^{2.7}$ (Cornell adjustment)[28]. LV ejection fraction was measured using a commercially available software program that applied Simpson's rule on the 2- and 4-chamber views. Stroke volume was obtained using the LV outflow Doppler method as the product between the outflow tract area and the LV output velocity integral[29].

The tricuspid annular plane systolic excursion (TAPSE) was calculated as the index of the RV global systolic function by determining the difference (in mm) between the end-diastolic and end-systolic measurements[30].

RV end-diastolic diameter was measured in the apical 4-chamber view at the basal, middle and apical levels in accordance with the protocol of Foale et al.[31].

Standard Doppler. Pulsed Doppler assessment of the LV inflow was performed in the apical 4-chamber view, with the sample volume placed at the level of the valve tips. The following measurements of the global LV diastolic function were determined: peak velocities of the E and A waves (m/s) and their ratio, deceleration time of the E wave (ms), isovolumic relaxation time (ms), measured as the time interval between the end of the systolic output flow and the onset of the transmitral E wave measured by placing the pulsed Doppler sample volume between the outflow tract and the mitral valve[32]. The pulsed Doppler RV diastolic indexes were determined in the apical 4-chamber view, placing the sample volume at the tips of the tricuspid valve. The following measurements of global RV filling were determined: E and A peak velocities (m/s), E/A ratio, and E wave deceleration time. The RV isovolumic relax-

ation time was measured in the parasternal long-axis view of the RV outflow tract, by measuring the time interval from the end of pulmonary LV outflow to the onset of tricuspid inflow[33]. Non-invasive measurement of the pulmonary artery systolic pressure was calculated in all the patients of the study using Doppler recordings of tricuspid regurgitation, using the modified Bernoulli equation. In particular, the pulmonary artery systolic pressure was considered as equal to 4 times the square of the peak velocity of the tricuspid jet, plus the right atrial pressure[34].

Pulsed Doppler myocardial imaging. Pulsed DMI was performed using spectral pulsed Doppler signal filters, adjusting the Nyquist limit until 15-20 cm/s (approximately equal to myocardial velocities), and using the minimal optimal gain. In the apical 4-chamber view, a 5 mm pulsed Doppler sample volume was placed at the level of the LV mitral annulus and RV tricuspid annulus. The apical view was chosen to obtain a quantitative assessment of the regional wall motion almost simultaneously to the Doppler inflow and outflow and to minimize the incidence angle between the Doppler beam and the longitudinal wall motion. Pulsed DMI is characterized by a myocardial systolic wave (S_m) and two diastolic waves – early (E_m) and atrial (A_m). The myocardial peak velocity of S_m (m/s), myocardial pre-contraction time (from the onset of ECG QRS complex to the beginning of S_m), and the contraction time (from the beginning to the end of the S_m wave) (all in ms) were calculated as systolic indexes. E_m and A_m peak velocities (m/s), the E_m/A_m ratio, and the regional relaxation time (RT_m) (ms) – the time interval between the end of S_m and the onset of E_m – were determined as diastolic measurements[22-26].

Statistical analysis. The analyses were performed using SPSS for Windows release 11.0 (Chicago, IL, USA). Variables are presented as mean ± SD. The Student's t-test for unpaired data was used to estimate differences between the two groups. The reproducibility of the measurements of the DMI parameters was determined in 20 subjects (10 SSc and 10 controls), in accordance with previously reported methods. The inter- and intraobserver variability was examined using Bland-Altman analysis. The 95% confidence limits of a single estimate of the measurements were calculated as $2*SD/\sqrt{2}$, and reported as a percent of the mean value. Linear regression analyses and a partial correlation test (either Pearson's or Spearman's method) were performed to assess univariate relations. Receiver-operating characteristic (ROC) curve analysis was performed to select optimal cut-off values of DMI measurements. Stepwise, forward, multiple regression analyses or logistic regression analyses were performed to weigh the independent effects of potential determinants on a dependent variable. Differences were significant at $p < 0.05$.

Results

Clinical characteristics of the study population. The two groups were comparable for age (56.3 ± 8.2 in SSc vs 55 ± 9.3 years in controls), gender (3 males/20 females vs 5 males/20 females), mean blood pressure (83.5 ± 4.5 vs 80.2 ± 3.3 mmHg), heart rate (78.1 ± 7.6 vs 76.9 ± 10.2 b/min), and body surface area (1.85 ± 0.11 vs 1.82 ± 0.08 m^2).

The skin thickness was quantified using the modified Rodnan skin score (mRSS), in accordance with the preliminary American College of Rheumatology criteria. SSc was classified as high mRSS (score ≥ 10; 11 patients) and low mRSS (score < 10; 12 patients). At chest CT, 11 patients showed interstitial pulmonary fibrosis. Immunofluorescence analysis detected an anticentromere antibody pattern in 8 patients, and anti-Scl-70 antibodies in 15 patients.

Standard Doppler echocardiographic analysis (Table I). LV mass index, diameters and ejection fraction were comparable between the two groups, while RV end-diastolic diameter was increased in SSc ($p < 0.01$). The tricuspid inflow peak E velocity and the E/A ratio were slightly decreased in SSc ($p < 0.01$), while systolic pulmonary artery pressure was increased ($p < 0.001$). In particular, 10 SSc patients (43.2%) had pulmonary hypertension (systolic pulmonary pressure > 35 mmHg).

Pulsed Doppler myocardial imaging analysis (Table II). DMI analysis detected, in SSc, impaired myocardial RV E_m peak velocities ($p < 0.001$), as well as a prolonged RT_m ($p < 0.001$) only at the level of the tricuspid annulus, even after correction for age, sex, heart rate, and body surface area (Fig. 1).

Systemic sclerosis subgroup analysis. We performed a separate subgroup DMI analysis dividing SSc patients according to whether they had a high (≥ 10) or low (< 10) mRSS. These measurements revealed that patients with greater skin involvement showed a more impaired RV myocardial diastolic function (RV E_m peak 0.118 vs 0.153 m/s in high vs low mRSS, $p < 0.0005$; RV RT_m 41.1 vs 33.6 ms in high vs low mRSS, $p < 0.01$).

Reproducibility of Doppler myocardial imaging measurements. The interobserver variability was ±2.6% for E_m peak velocity, ±3.2% for S_m peak velocity and ±4.2% for RT_m. The intraobserver variability was similar: ±2.2% for E_m peak velocity, ±3.0% for S_m peak velocity, ±3.8% for RT_m.

Univariate relations of Doppler myocardial imaging indexes. In the SSc group, E_m peak velocity of the tricuspid annulus was inversely related to both the Rodnan skin score and systolic pulmonary pressure (Figs. 2 and

Table I. Standard Doppler echocardiographic comparison between the two groups.

Variable	SSc	Controls	p
Left ventricle			
Septal wall thickness (mm)	9.8 ± 3.2	9.7 ± 0.8	NS
Posterior wall thickness (mm)	8.4 ± 1.1	8.3 ± 1.2	NS
End-diastolic diameter (mm)	47.4 ± 3.7	49.4 ± 3.2	NS
End-systolic diameter (mm)	27.0 ± 4.7	30.8 ± 1.9	NS
Endocardial fractional shortening (%)	38.7 ± 4.7	39.2 ± 6.2	NS
Stroke volume (ml)	64.7 ± 12.5	69.6 ± 6.9	NS
Mass index ($g/m^{2.7}$)	64 ± 9.7	60.6 ± 5.5	NS
Mitral peak E velocity (m/s)	0.68 ± 0.09	0.71 ± 0.2	NS
Mitral peak A velocity (m/s)	0.66 ± 0.06	0.68 ± 0.1	NS
Mitral peak E/A ratio	1.04 ± 0.4	1.2± 0.8	NS
Mitral deceleration time (ms)	164.4 ± 30.9	162.1 ± 14.8	NS
Mitral IVRT (ms)	82.0 ± 10.5	78.5 ± 9.7	NS
Right ventricle			
Wall thickness (mm)	5.1 ± 0.4	4.3 ± 1.2	NS
Outflow tract (mm)	26.4 ± 2.2	21.2 ± 3.8	< 0.001
TAPSE (mm)	19.1 ± 3.5	20.1 ± 2.6	NS
Tricuspid peak E velocity (m/s)	0.57 ± 0.2	0.64 ± 0.1	< 0.05
Tricuspid peak A velocity (m/s)	0.45 ± 0.09	0.46 ± 0.2	NS
Peak E/A ratio	1.21 ± 0.09	1.49 ± 0.56	< 0.01
Tricuspid deceleration time (ms)	128.2 ± 9.2	120.8 ± 8.5	NS
Tricuspid IVRT (ms)	79.8 ± 11.2	76.8 ± 9.2	NS
Pulmonary artery systolic pressure (mmHg)	44.2 ± 9.8	21.2 ± 5.8	< 0.001

IVRT = isovolumic relaxation time; SSc = systemic sclerosis; TAPSE = tricuspid annular plane systolic excursion.

Table II. Doppler myocardial imaging analysis of the mitral and tricuspid annuli.

Variable	SSc	Controls	p
Mitral annulus			
S_m peak (m/s)	0.15 ± 0.02	0.16 ± 0.03	NS
Q-S_m (ms)	77.2 ± 10.7	74.7 ± 12.3	NS
CT_m (ms)	259.7 ± 13.2	250 ± 13.5	NS
E_m peak (m/s)	0.18 ± 0.03	0.20 ± 0.04	NS
A_m peak (m/s)	0.10 ± 0.02	0.11 ± 0.01	NS
E_m/A_m ratio	1.9 ± 0.6	1.8 ± 0.5	NS
RT_m (ms)	63.4 ± 12.9	59.2 ± 10.6	NS
Tricuspid annulus			
S_m peak (m/s)	0.12 ± 0.03	0.12 ± 0.01	NS
Q-S_m (ms)	89.2 ± 8.9	75.6 ± 8.2	< 0.001
CT_m (ms)	243 ± 58	240.6 ± 55.3	NS
E_m peak (m/s)	0.13 ± 0.03	0.20 ± 0.05	< 0.0001
A_m peak (m/s)	0.14 ± 0.5	0.09 ± 0.01	< 0.001
E_m/A_m ratio	0.92 ± 0.38	2.2 ± 0.5	< 0.0001
RT_m (ms)	42.8 ± 7.8	18.8 ± 6.1	< 0.0001

A_m = atrial myocardial diastolic wave; CT_m = myocardial contraction time; E_m = early myocardial diastolic wave; Q-S_m = myocardial pre-contraction time; RT_m = myocardial relaxation time; S_m = myocardial systolic peak velocity; SSc = systemic sclerosis.

3). Conversely, RV RT_m appeared to be directly related to the same parameters (Figs. 2 and 3). The negative correlation between skin involvement and RV E_m peak velocity was observed even in the subgroup of SSc patients without detectable pulmonary hypertension or fibrosis (Fig. 4). In addition, close associations were observed between the severity of interstitial pulmonary fibrosis as assessed using CT scan and both RV E_m (ρ = -0.73, $p < 0.0005$) and RV RT_m ($\rho = 0.69$, $p < 0.001$). RV E_m peak velocity was also inversely associated with the presence of the anti-Scl-70 antibody pattern.

Multivariate analysis. Stepwise forward, multiple linear regression or logistic regression analyses were performed in the SSc group to weigh the independent associations between the RV myocardial parameters and other clinical or instrumental features of the disease. Using these models, in SSc patients the independent inverse association of RV E_m peak velocity with both the Rodnan skin score (β coefficient = -0.62, $p < 0.0005$) and pulmonary systolic pressure (β coefficient = 0.71, $p < 0.0001$) as well as the independent inverse correlation of the same RV E_m peak velocity with the severity of interstitial pulmonary fibrosis (odds ratio 0.68, 95% confidence interval 0.45-0.83, $p < 0.0005$) were confirmed even after adjusting for potential determinants such as age, sex, body surface area, heart rate, ventricular diameters and wall thicknesses. In addition, RV E_m was an independent predictor of the anti-Scl-70 antibody pattern (odds ratio 0.68, 95% confidence interval 0.45-0.83, $p < 0.01$).

Sensitivity and specificity of standard Doppler and Doppler myocardial imaging. The sensitivity and specificity of DMI-measured E_m peak velocity of the tricuspid annulus was determined to compare patients with either diffuse or limited cutaneous SSc. A cut-off point of DMI RV E_m peak velocity < 0.11 m/s (ROC curve) well differentiated SSc patients with a high Rod-

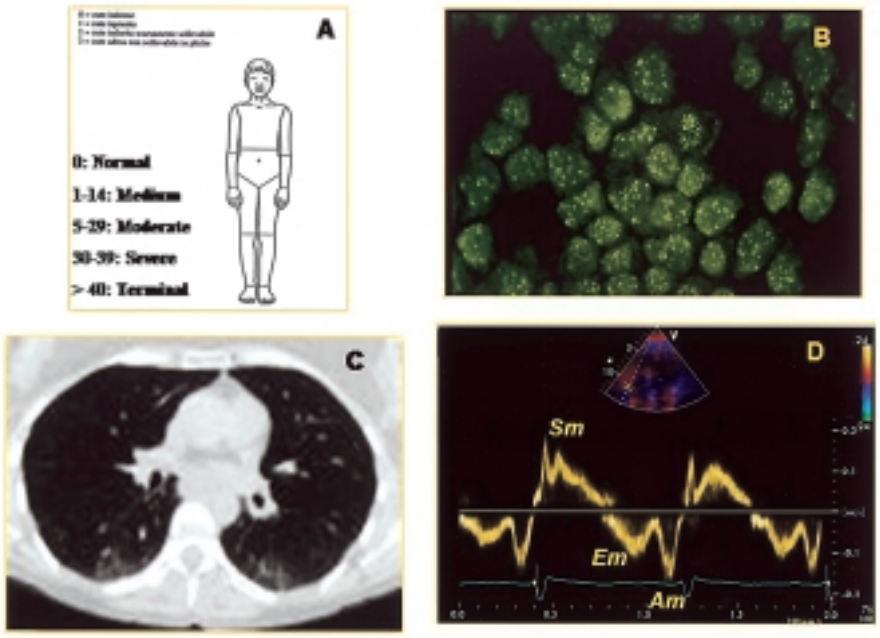

Figure 1. *Systemic sclerosis patient.* A: *modified Rodnan skin score, used to quantify the skin involvement;* B: *immunofluorescence analysis for the detection of the anti-topoisomerase antibody pattern;* C: *high-resolution chest computed tomography scan showing interstitial pulmonary fibrosis;* D: *Doppler myocardial imaging pattern of the tricuspid annulus showing an impaired early diastolic function (E_m/A_m ratio < 1). A_m = myocardial atrial diastolic wave; E_m = myocardial early diastolic wave; S_m = myocardial systolic peak velocity.*

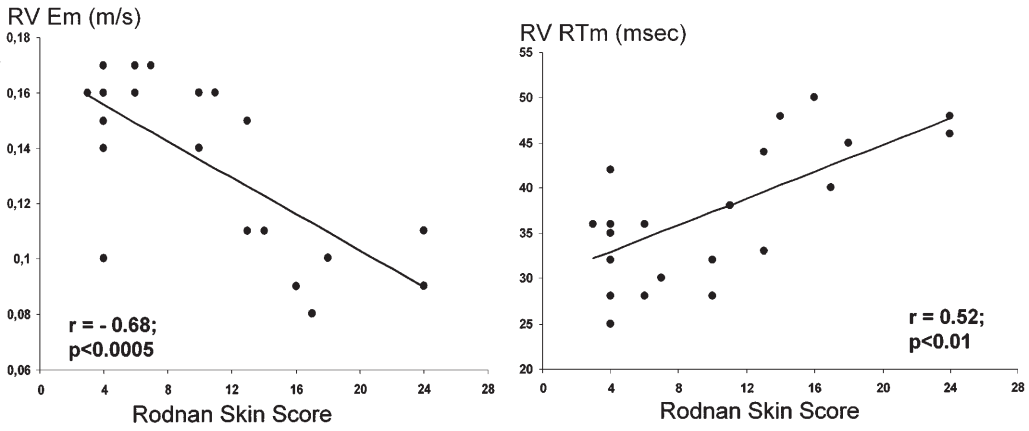

Figure 2. *Scatter plots of both right ventricular myocardial early diastolic wave (RV E_m) peak velocity and right ventricular myocardial relaxation time (RV RT_m) using the modified Rodnan skin score in the systemic sclerosis group.*

nan skin score (sensitivity 89%, specificity 90%; area under the curve 0.96), interstitial pulmonary fibrosis (sensitivity 89%, specificity 91%; area under the curve 0.95) and pulmonary hypertension (sensitivity 88%, specificity 82%; area under the curve 0.92). What is more, the same cut-off value of RV E_m was able to predict the presence of the anti-Scl-70 antibody pattern at serological analysis (Fig. 5).

Discussion

SSc is a multisystem disorder characterized by widespread vascular lesions and fibrosis of the skin and specific internal organs. Cardiac involvement is a common finding in SSc, but is often clinically occult. In fact, clinical evidence of myocardial disease may be found in 20-25% of patients with SSc, while at *post-mortem* examination the heart is found to be involved in up to 80% of patients. A diagnosis of a subclinical cardiac involvement may be therefore essential for adequate long-term management of such patients[6,10,11].

Although several reports have previously described the global diastolic function in SSc by means of standard Doppler echocardiography[9], myocardial perfusion single-photon emission CT[15] and integrated backscatter[13], little is known about DMI myocardial patterns in such patients[10]. The present study underscores the use-

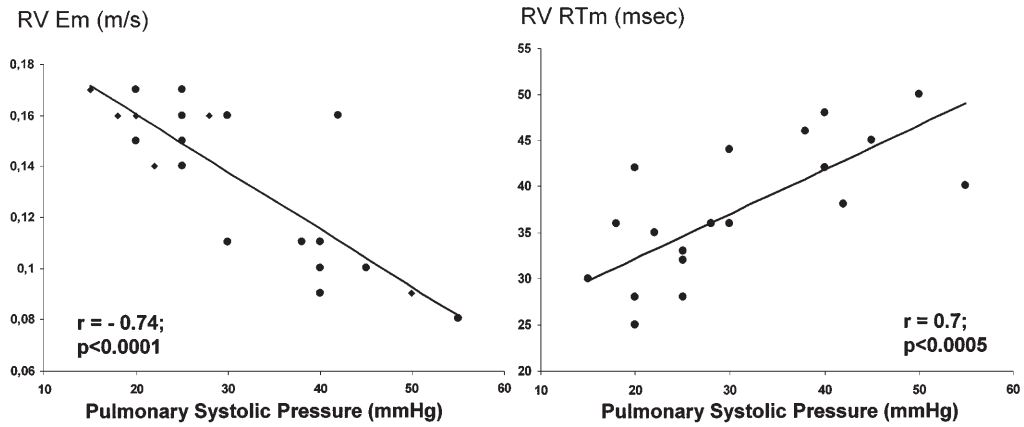

Figure 3. *Scatter plots of both right ventricular myocardial early diastolic wave (RV E_m) peak velocity and right ventricular myocardial relaxation time (RV RT_m) and Doppler-measured pulmonary systolic pressure in the systemic sclerosis group.*

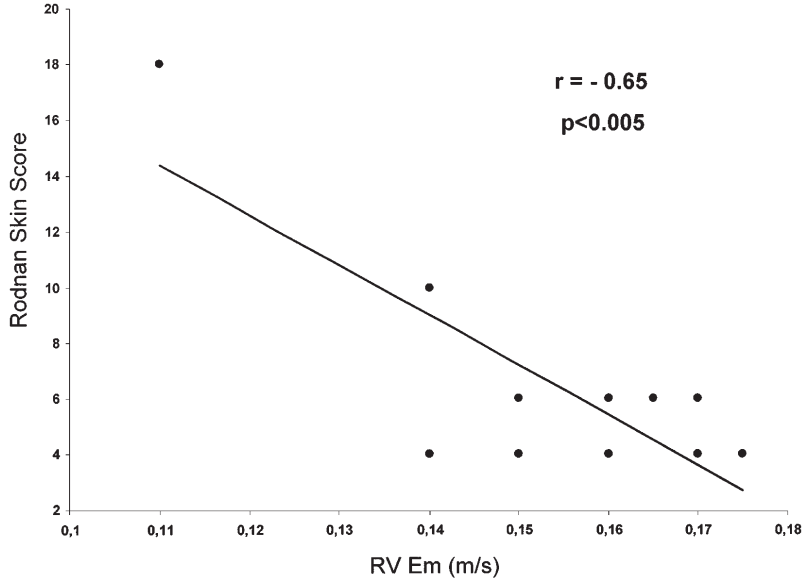

Figure 4. *Scatter plots of the negative correlation between skin involvement and right ventricular myocardial early diastolic wave (RV E_m) peak velocity in the subgroup of systemic sclerosis patients without detectable pulmonary hypertension or fibrosis.*

fulness of pulsed DMI to assess RV myocardial function in SSc patients without clinically evident cardiac disease in whom no other cause of diastolic dysfunction was detected. To the best of our knowledge, this is the first attempt to assess RV involvement in SSc using this technique.

Experimental studies have reported that in normal conditions the right ventricle, unlike the left, begins to eject after a minimal isovolumic systolic contraction time, and starts its diastolic filling without an isovolumic relaxation interval, since it works against a lower vascular impedance[16,17]. However, the present study emphasizes early RV diastolic dysfunction in patients with SSc since significantly lower early diastolic peak velocities and prolonged relaxation time intervals were observed at the level of the tricuspid annulus, despite slightly reduced Doppler measurements. Conversely, LV myocardial indexes in the two groups were comparable.

In our experience we have found, using DMI, prolonged RT_m and decreased RV myocardial peak velocities in several pathologic conditions involving the right ventricle. These anomalies were related to either the increased pulmonary load or to intrinsic RV myocardial dysfunction[19,24-26,35,36].

As for the RV regional systolic function, SSc patients showed, at the level of the tricuspid annulus, normal systolic peak velocities and prolonged pre-contraction times even after correction for age and heart rate. Vogel et al.[37] reported that in an animal model myocardial acceleration during isovolumic contraction, an index comparable to our myocardial pre-contraction time, was a sensitive indicator of the RV contractile function unaffected by preload and afterload changes

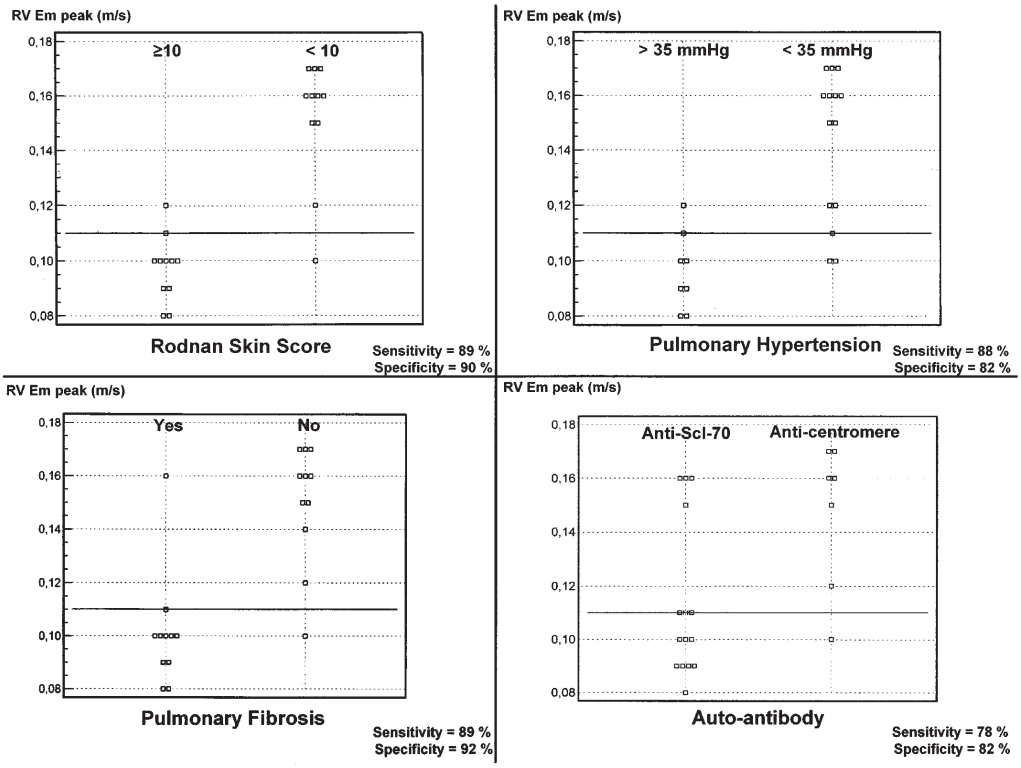

Figure 5. *Interactive plot diagrams (receiver-operating characteristic curve analysis) of right ventricular myocardial early diastolic wave (RV E_m) peak velocity in systemic sclerosis patients. For RV E_m velocity, a cut-off point < 0.11 m/s showed a high sensitivity and specificity for the detection of more severe skin and pulmonary involvement, as well as of the serological antibody pattern with the worst long-term prognosis (anti-Scl-70).*

and able to measure the force-frequency relation. The prolongation of such a systolic myocardial parameter in our population of SSc patients is therefore suggestive of an early impairment even of the RV myocardial contractile function, despite normal TAPSE measurements.

Of note, in our population of SSc patients, RV E_m peak velocity (inversely) and RT_m (directly) were both significantly related to the pulmonary systolic pressure, the severity of pulmonary interstitial fibrosis and to the mRSS. In addition, a parallel impairment of both the skin and RV diastolic regional function was observed even in patients without detectable pulmonary hypertension or fibrosis. These correlations indicate how an impaired RV regional diastolic function and relaxation may occur simultaneously with the skin involvement and the increase in systolic pulmonary pressure. Multivariate analysis provided further information about this association by adjusting for several confounders, chosen according to the heart physiology. By this model, RV E_m peak velocity was the only independent determinant of the Rodnan skin score, pulmonary systolic pressure and pulmonary fibrosis, and a RV E_m peak velocity < 0.11 m/s selected SSc patients with more severe skin involvement, pulmonary hypertension and fibrosis with a high sensitivity and specificity.

The main involvement of the RV wall as well as the close relationship of the RV regional dysfunction with pulmonary hypertension suggest that myocyte hypoxia with a consequently impaired intracellular calcium transport may determine sufferance in diastolic relaxation secondary to pulmonary pressure overload[5,23].

On the other hand, a previous report demonstrated that both systolic and early diastolic regional velocities evaluated by DMI are directly dependent on the myocardial structure, characterized by the percent of interstitial fibrosis and the myocardial beta-adrenergic receptor density assessed by endomyocardial biopsy[38]. Therefore, as recently confirmed in the invasive analysis of Fernandes et al.[14], which identified cardiac remodeling characterized by diffuse myocardial fibrin deposits in SSc patients, in our patients the RV myocardial function could have been further impaired by a direct involvement of the ventricular walls by the myopathic process.

Study limitations. Our study has some limitations. The first one, intrinsic to the Doppler technique, is the angle dependence of pulsed DMI and the possible presence of artifacts. However, we used the same angle incidence of transmitral Doppler and our DMI reproducibility was good. We also have to point out that the overall cardiac motion in space influences DMI regional velocities, thus limiting the evaluation of myocardial heterogeneity[22]. In our study, however, the concept of impaired myocardial function in SSc arises from the comparison of the regional DMI variables between the two different groups.

Besides, the gold standard for the assessment of the diastolic function and pulmonary artery pressure is based on invasive methods. An assessment of the systolic pulmonary artery pressure by heart catheterization might have provided more accurate information about RV and right atrial pressures in our patients. However, a number of studies have pointed out that pulmonary hypertension may be accurately determined by means of Doppler-measured tricuspid regurgitation[5,6].

Also, the data of the present study may not be extrapolated to the overall population of SSc patients because of the exclusion of severe heart failure classes which may have eliminated patients with advanced systolic impairment from statistical analyses. However, we intentionally selected relatively asymptomatic patients in order to examine the early changes of the DMI regional diastolic properties in SSc.

Finally, our SSc population includes a small number of male patients. However, this is in accordance with the general epidemiological features of the disease[1,2]. What is more, the control group was sex-comparable, and excluding 3 male patients from the analysis did not change the results.

Clinical implications. The present study proposes that pulsed DMI could represent a valuable non-invasive and easily repeatable tool for the evaluation of the RV involvement in SSc. The relationships of the RV myocardial diastolic dysfunction with both the skin and pulmonary involvement as well as with the serum antibody pattern emphasizes the ability of DMI to identify patients with a more diffuse and severe form of SSc.

Further longitudinal studies using DMI will be needed to follow the progression from early RV myocardial impairment to the onset of RV chamber dysfunction and the development of overt congestive heart failure. This issue may be critical for the early identification of SSc patients who are at a higher risk of cardiac and pulmonary impairment, ideally when they are still asymptomatic prior to the development of severe vasculopathy, when it may be most feasible to modify the disease process using new potential therapies.

Acknowledgments

The authors are grateful to Mrs. Celeste Perillo and Mrs. Michela Ibelli for excellent nursing and technical support.

References

1. Sub-committee for Scleroderma Criteria of the American Rheumatism Association Diagnostic Therapeutic Criteria Committee. Preliminary criteria for the classification of systemic sclerosis (scleroderma). Arthritis Rheum 1980; 23: 581-90.
2. Le Roy EC, Black C, Fleischmajer R, et al. Scleroderma (systemic sclerosis): classification, subsets and pathogenesis. J Rheumatol 1988; 15: 202-5.
3. Clements P, Lachenbruch P, Seibold JR, et al. Inter and intraobserver variability of total skin thickness score (modified Rodnan TSS) in systemic sclerosis. J Rheumatol 1995; 22: 1281-5.
4. Akesson A, Fiori G, Krieg T, van den Hoogen FH, Seibold JR. Assessment of skin, joint, tendon and muscle involvement. Clin Exp Rheumatol 2003; 21 (Suppl 29): S5-S8.
5. Denton CP, Cailes JB, Phillips GD, Wells AJ, Black CM, Bois RM. Comparison of Doppler echocardiography and right heart catheterization to assess pulmonary hypertension in systemic sclerosis. Br J Rheumatol 1997; 36: 239-43.
6. Mukerjee D, St George D, Knight C, et al. Echocardiography and pulmonary function as screening tests for pulmonary arterial hypertension in systemic sclerosis. Rheumatology (Oxford) 2004; 43: 461-6.
7. Montisci R, Vacca A, Garau P, et al. Detection of early impairment of coronary flow reserve in patients with systemic sclerosis. Ann Rheum Dis 2003; 62: 890-3.
8. Sulli A, Ghio M, Bezante GP, et al. Blunted coronary flow reserve in systemic sclerosis. Rheumatology (Oxford) 2004; 43: 505-9.
9. Giunta A, Tirri E, Maione S, et al. Right ventricular diastolic abnormalities in systemic sclerosis. Relation to left ventricular involvement and pulmonary hypertension. Ann Rheum Dis 2000; 59: 94-8.
10. Plazak W, Zabinska-Plazak E, Wojas Pelc A, et al. Heart structure and function in systemic sclerosis. Eur J Dermatol 2002; 12: 257-62.
11. Steen V. The heart in systemic sclerosis. Curr Rheumatol Rep 2004; 6: 137-40.
12. Aguglia G, Sgreccia A, Bernardo ML, et al. Left ventricular diastolic function in systemic sclerosis. J Rheumatol 2001; 28: 1563-7.
13. Hirooka K, Naito J, Koretsune Y, et al. Analysis of transmural trends in myocardial integrated backscatter in patients with progressive systemic sclerosis. J Am Soc Echocardiogr 2003; 16: 340-6.
14. Fernandes F, Ramires FJ, Arteaga E, Ianni BM, Bonfa ES, Mady C. Cardiac remodeling in patients with systemic sclerosis with no signs or symptoms of heart failure: an endomyocardial biopsy study. J Card Fail 2003; 9: 311-7.
15. Nakajima K, Taki J, Kawano M, et al. Diastolic dysfunction in patients with systemic sclerosis detected by gated myocardial perfusion SPECT: an early sign of cardiac involvement. J Nucl Med 2001; 42: 183-8.
16. Santamore WP, Dell'Italia LJ. Ventricular interdependence: significant left ventricular contributions to right ventricular systolic function. Prog Cardiovasc Dis 1998; 40: 289-308.
17. Myhre ES, Slinker BK, LeWinter MM. Absence of right ventricular isovolumic relaxation in open-chest anesthetized dogs. Am J Physiol 1992; 263 (Part 2): H1587-H1590.
18. Yu CM, Sanderson JE, Chan S, Yeung L, Hung YT, Wook S. Right ventricular diastolic dysfunction in heart failure. Circulation 1996; 93: 1509-14.
19. D'Andrea A, Caso P, Severino S, et al. Different involvement of right ventricular myocardial function in either physiologic or pathologic left ventricular hypertrophy: a Doppler tissue study. J Am Soc Echocardiogr 2003; 16: 154-61.
20. Douglas PS, O'Toole ML, Hiller WD, Reichek N. Different effects of prolonged exercise on the right and left ventricles. J Am Coll Cardiol 1990; 15: 64-9.
21. Henriksen E, Landelius J, Kangro T, et al. An echocardiographic study of right and left ventricular adaptation to

physical exercise in elite female orienteers. Eur Heart J 1999; 20: 309-16.
22. Isaaz K, Thompson A, Ethevenot G, Cloez JL, Brembilla R, Pernot C. Doppler echocardiographic measurement of low velocity motion of the left ventricular posterior wall. Am J Cardiol 1989; 64: 66-75.
23. Severino S, Caso P, Galderisi M, et al. Use of pulsed Doppler tissue imaging to assess regional left ventricular diastolic dysfunction in hypertrophic cardiomyopathy. Am J Cardiol 1998; 82: 1394-8.
24. D'Andrea A, Caso P, Galderisi M, et al. Assessment of myocardial response to physical exercise in endurance competitive athletes by pulsed Doppler tissue imaging. Am J Cardiol 2001; 87: 1226-30.
25. D'Andrea A, Ducceschi V, Caso P, et al. Usefulness of Doppler tissue imaging for the assessment of right and left ventricular myocardial function in patients with dual-chamber pacing. Int J Cardiol 2001; 81: 75-83.
26. Caso P, Galderisi M, Cicala S, et al. Association between myocardial right ventricular relaxation time and pulmonary arterial pressure in chronic obstructive lung disease: analysis by pulsed Doppler tissue imaging. J Am Soc Echocardiogr 2001; 14: 970-7.
27. Devereux RB, Reicheck N. Echocardiographic determination of left ventricular mass: anatomic validation of the method. Circulation 1977; 55: 613-8.
28. de Simone G, Daniels SR, Devereux RB, et al. Left ventricular mass and body size in normotensive children and adults: assessment of allometric relations and impact of overweight. J Am Coll Cardiol 1992; 20: 1251-60.
29. Dubin J, Wallerson DC, Cody RJ, Devereux RB. Comparative accuracy of Doppler echocardiographic methods for clinical stroke volume determination. Am Heart J 1990; 120: 116-23.
30. Kaul S, Tei C, Hopkins JM, Shah PM. Assessment of right ventricular function using two-dimensional echocardiography. Am Heart J 1984; 107: 526-31.
31. Foale R, Nihoyannopoulos P, McKenna W, et al. Echocardiographic measurement of normal adult right ventricle. Br Heart J 1986; 56: 33-44.
32. Quinones MA. How to assess diastolic function by Doppler echocardiography. In: Braunwald E, ed. Heart disease, update. Philadelphia, PA: WB Saunders, 1993: 351-8.
33. Larrazet F, Pellerin D, Fournier C, Witchitz S, Veyrat C. Right and left isovolumic ventricular relaxation time intervals compared in patients by means of a single-pulsed Doppler method. J Am Soc Echocardiogr 1997; 10: 699-706.
34. Tramarin R, Torbicki A, Marchandise B, Laaban JP, Morpurgo M. Doppler echocardiographic evaluation of pulmonary artery pressure in chronic obstructive pulmonary disease. A European multicentre study. Working Group on Noninvasive Evaluation of Pulmonary Artery Pressure. European Office of the World Health Organization, Copenhagen. Eur Heart J 1991; 12: 103-11.
35. D'Andrea A, Caso P, Sarubbi B, et al. Right ventricular myocardial activation delay in adult patients with right bundle branch block late after repair of tetralogy of Fallot. Eur J Echocardiogr 2004; 5: 123-31.
36. D'Andrea A, Caso P, Sarubbi B, et al. Right ventricular myocardial dysfunction in adult patients late after repair of tetralogy of Fallot. Int J Cardiol 2004; 94: 213-20.
37. Vogel M, Schmidt MR, Kristiansen SB, et al. Validation of myocardial acceleration during isovolumic contraction as a novel noninvasive index of right ventricular contractility: comparison with ventricular pressure-volume relations in an animal model. Circulation 2002; 105: 1693-9.
38. Shan K, Bick RJ, Poindexter BJ, et al. Relation of tissue Doppler derived myocardial velocities to myocardial structure and beta-adrenergic receptor density in humans. J Am Coll Cardiol 2000; 36: 891-6.